Modeling the Thermal Decomposition of Chrysotile

John P. Sanders and Denis A. Brosnan
The National Brick Research Center
Clemson University
Clemson, South Carolina, USA

Abstract

While the health effects of asbestos exposure have been known since the 1960's, there remains great interest in the identity of residuals of asbestos species after exposure to high temperatures. It is of interest to determine potential exposure to fiber form asbestos during demolition of furnace linings after the asbestos has been exposed to high temperatures for an extended period of time.

It is well known that asbestos minerals exhibit dehydroxylation at moderate temperatures followed by eventual recrystallization to another crystal structure at elevated temperatures. Chrysotile asbestos, for example, is reported in most authoritative references to dehydroxylate at about 660^{o}C followed by recrystallization forming forsterite above 800^{o}C. However, dehydroxylation of chrysotile at lower temperatures has been reported. As the kinetics of the dehydroxylation determine the potential for exposures in furnace demolition, research was initiated with chrysotile.

A combination of traditional thermal analysis (TG and DSC) along with evolved gas analysis by FTIR was used to study the thermal decomposition of the minerals. Evolved gas analysis was used to identify reaction products during dehydroxylation and from carbonate minerals included in the asbestos. A kinetic model for dehydroxylation was established, and residuals after thermal analysis tests were identified using X-ray Diffraction (XRD).

1. Introduction

The health effects associated with the exposure to chrysotile are well known and have been documented in several sources. The health dangers of chrysotile revolve around its fibrous morphology. These fibers tend to implant into the lungs and are associated with an array of diseases including asbestosis, lung cancer and mesothelioma [1]. Chrysotile asbestos was used for many years as insulation in industrial process equipment. It is well known that asbestos decomposes upon exposure to temperatures greater than 400°C depending on the exposure time [2]. After decomposition and the eventual recrystallization, several new phases, such as forsterite, have been reported.

In order to estimate the extent of worker exposure, a kinetic study of the decomposition of chrysotile was undertaken. The development of the kinetic models allows for prediction of exposure to chrysotile based on the thermal history of the particular industrial process. Of particular interest in this study was the development of the forsterite phase for which no negative epidemiological data exists. It was determined that forsterite begins to form during the decomposition of the chrysotile mineral and was the only detectable phase on heating to 900°C.

There are several proposed reaction models for the decomposition of chrysotile [3,4,5]. Chrysotile exhibits a weight loss during thermogravimetric analysis, TG, and an associated endothermic peak due to the dehydroxylation or loss of crystalline water from the mineral above 500°C during calorimetric (DSC) analysis. At temperatures above 800°C, there is a sharp exotherm that is associated with the formation of forsterite (Mg_2SiO_4). It is unclear from the proposed models if forsterite is formed immediately as the product of dehydroxylation or only at higher temperature, after the exotherm. The decomposition path proposed by Gualtieri and Tartaglia, which suggests an amorphous intermediate phase, is given in equation 1 [4].

$Mg_3(OH)_4Si_2O_5$ (Chrysotile) → (<500°C) $Mg_3Si_2O_7$(Metachrysotile) + H_2O →
(<800°C) Mg2SiO4 (Forsterite) + MgSiO3 (Enstatite) [Equation 1]

According to Grimshaw, forsterite forms first, during the large exotherm and enstatite only forms after heating to temperatures greater than 1100°C [5].

Finally, Khorami et al. and Gallagher proposed a simpler reaction mechanism where forsterite is formed as a result of dehydroxylation [3]. This reaction path is given in equation 2.

$$Mg_3(OH)_4Si_2O_5 \text{ (Chrysotile)} \rightarrow (<500°C)\ Mg2SiO4 \text{ (Forsterite)} + SiO_2 \text{ (Silica)} + 4H_2O \quad \text{[Equation 2]}$$

The temperatures at which dehydroxylation and forsterite recrystallization occur are known to be influenced by the heating rate used for the analysis [1,3]. This implies that with very long exposure time, a high degree of decomposition can be expected at relatively low temperatures as suggested by Dodd [2]. The predicted behavior for very long exposure times will be evaluated using the kinetic models developed in this study.

Chrysotile is a hydrated magnesium silicate from the serpentine mineral family. Chrysotile is composed of stacks of brucite, $[Mg_6O_4(OH)_8]^{4-}$, octahedral sheets between silica, $(Si_4O_{10})^{4-}$, tetrahedral sheets. The fibrous habit of chrysotile is derived from a mismatch between the lattice dimensions of the sheets and results in rolled structure. Furthermore, chrysotile is mined as fiber bundles in parent rock. To remove and refine the chrysotile, the parent rock must be crushed and separated. This typically results in some remnant of the parent rock or contamination in the chrysotile. Common impurities are listed in Table 1 along with their characteristic decomposition temperature [3,5].

Table 1 – Common Impurity Minerals

Mineral Name	Formula	Characteristic Decomposition Temperature (DTA Peak) °C
Brucite	$Mg(OH)_2$	435°C
Magnesite	$MgCO_3$	760°C
Dolomite	$MgCO_3 \bullet CaCO_3$	770°C, 870°C
Calcite	$CaCO_3$	880°C
Talc	$Mg_3Si_4O_{10}(OH)_2$	910°C
Magnetite	Fe_3O_4	

2. Materials and Methods

The material used in this study was derived from the NIST (National Institute of Standards and Technology) SRM (Standard Reference Material) 1866a, which is a set of typical asbestos minerals including chrysotile, and two amphibole asbestos minerals along with a glass fiber reference. For this study only the chrysotile sample was used. According to the test certificate, this material is greater than 90% chrysotile. The theoretical weight loss for chrysotile is 13%. In this study an average weight loss of 12.8% was observed which indicates a somewhat higher level of purity.

The X-ray diffraction pattern was also obtained on the unground fibers of SRM 1866A using a Scintag X-ray diffraction unit. The sample was rotated during the analysis relative to the X-ray path to avoid preferential orientation. A step size of 0.02° was used with a collection time of 2 seconds per step over a range of 10 to 75° with copper K_α radiation. The samples not ground for any of the analysis to avoid preferential dehydroxylation of the fiber edges [1]. Only peaks for clinochrysotile (JCPDS 31-0808) were detected [4].

To study the kinetics of the dehydroxylation of chrysotile and the recrystallization of forsterite, a series of heating experiments were performed in a Netzsch STA 449 C with a TG/DSC sample carrier with open alumina crucibles. Heating rates from 1, 2, 4, 8, 16, and 32°C min^{-1} were used for the evaluation. In some cases, evolved gas analysis by coupled FTIR was used to identify the presence of trace amounts of impurity phases [3]. A sample size of 27 ± 1 mg was used for this study. The unground fibers were lightly packed into the alumina crucibles to ensure good thermal contact for the DSC measurements. A flowing atmosphere, 100 ml min^{-1}, of 80% N_2 and 20% O_2 was used for this evaluation

3. Thermal Analysis of Chrysotile Mineral

An example of the thermal behavior of the chrysotile mineral used in this study is given in Figure 1 for a sample heated at 8°C min^{-1}. There was an initial small weight loss due to adsorbed water around 100°C which was followed by a large weight loss with an onset of 616°C which was due to the dehydroxylation of the chrysotile mineral. For the DSC signal, a large endotherm with peaks at 636 and 689°C was observed. Likewise, the DTG (derivative of the weight loss) curve also showed a two-humped peak, as did the H_2O trace from the FTIR. The two stages of the dehydroxylation reaction seen in the DTG, DSC and H_2O traces have also been observed by Khorami et al., who associated this behavior with the preferential decomposition of the fiber edges as opposed to the bulk of the fiber [3]. Accordingly, this preferential weight loss becomes more pronounced as the fiber length increases. Lastly, a large exotherm with a peak of 821°C was observed which is associated with the crystallization of forsterite.

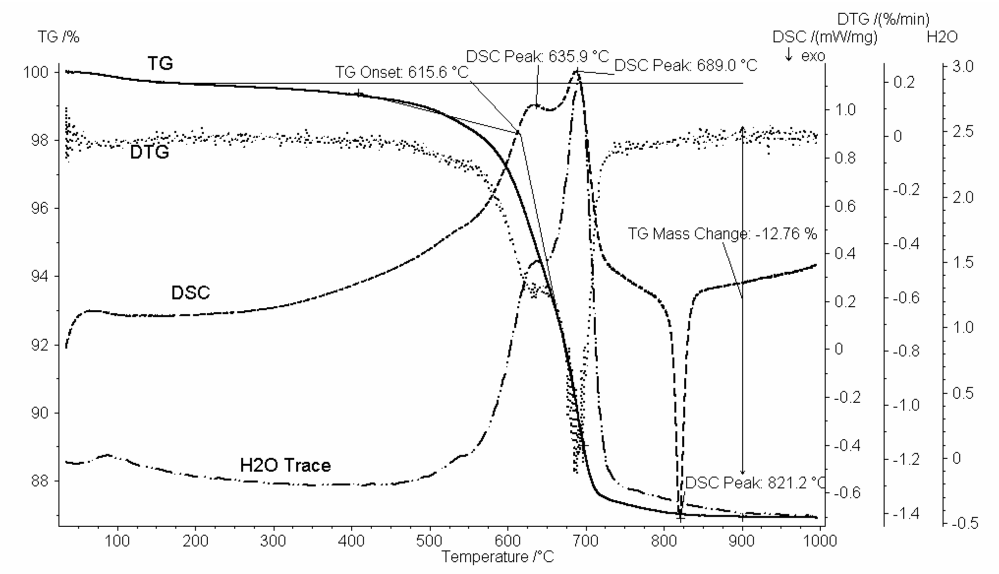

Figure 1 – TG/DSC at 8°C min^{-1}

The effect of heating rate on the onset of dehydroxylation and the forsterite recrystallization is given in Table 2. The onset temperature of the TG data due to the dehydroxylation of the chrysotile was strongly influenced by the heating rate. For the heating rates used in this study which ranged from 1°C min^{-1} to 32°C min^{-1}, the onset temperature varied by approximately 100°C with slower heating rates giving lower onset temperature as would be expected. For the endothermic DSC peak associated with dehydroxylation, two peaks have been reported. As has been discussed, the first peak was due to the preferential decomposition of the fiber edges, and the second peak was due to the decomposition of the bulk of the fiber. For the slower heating rates (1 and 2°C min^{-1}), the second DSC peak was not resolved but appeared as a small shoulder on the DSC peak. Evolved gas analysis by FTIR was only obtained for heating rates above 8°C min^{-1} due to limitations on cooling the MCT detector of the FTIR below its curie temperature for the extended time required for the slower heating rates.

For the exothermic DSC peak associated with the recrystallization of forsterite given in Table 2, there was less of a dependence on the heating rate. For the range of heating rates used in this study the peak temperatures only had a range of about 40°C. It is clear from this data that the dehydroxylation is much more strongly influenced by the rate of temperature increase than is the recrystallization exotherm.

Table 2 – Decomposition and Recrystallization Data

Heating Rate	**Onset of Dehydroxylation (TG Data) °C**	**Dehydroxylation Peak Temperature (DSC Data) °C**	**Onset of H_2O Emission (FTIR Data) °C**	**Forsterite Recrystallization Peak (DSC Data) °C**
1°C min^{-1}	565.6	575.5	Not Determined	799.3
2°C min^{-1}	585.5	592.4	Not Determined	805.8
4°C min^{-1}	606.0	617.2, 668.4	Not Determined	813.3
8°C min^{-1}	629.8	635.9, 689.0	569.5	821.2
16°C min^{-1}	641.9	654.0, 706.8	587.1	829.1
32°C min^{-1}	660.0	680.7, 727.5	604.9	838.1

To identify the presence of impurity phases such as those listed in Table 1, a slightly higher heating rate, 16°C min^{-1} was used to enhance the CO_2 peaks. This analysis is displayed in Figure 2. A broad CO_2 evolution was observed in the range of 200 to 600°C. This emission was probably due to the evolution of CO_2 adsorbed on the fiber surfaces, but has been attributed to the decomposition of “mixed carbonates of low relative stability”, by Khorami et al [3]. Two very small evolutions of CO_2 were observed with peak emissions at 711°C and 818°C. These peaks are likely related to the presence of trace amounts of magnestie and calcite respectively.

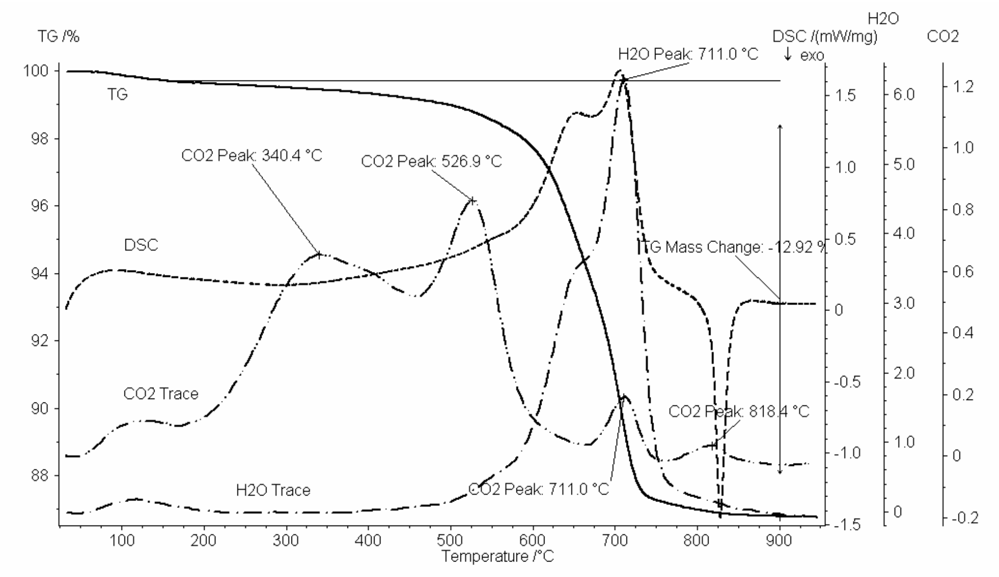

Figure 2 – TG/DSC/FTIR at 16°C min^{-1}

Again a large evolution of H_2O was observed due to the dehydroxylation of the chrysotile mineral. A comparison of the H_2O evolution is given in Figure 3 for several heating rates. The H_2O evolution also showed the two-stage nature of the chrysotile decomposition. Both the onset of and peak H_2O emission were strongly affected by increasing heating rate. While the dehydroxylation is clearly a two-step process, the first H_2O evolution peak was less resolved from the second, larger H_2O evolution at higher heating rates. The data provided from the evolved gas analysis will be used to develop and rationalize the kinetic model that will be described in a subsequent section.

A sample was also analyzed by X-ray diffraction after heating to 900°C, which is above the exotherm attributed to forsterite recrystallization. Only peaks for forsterite were detected in this sample. To identify forsterite, JCPDS file 31-0189 was used for identification [4]. No enstatite or silica phases were detected in the X-ray diffraction pattern for the sample heated to 900°C.

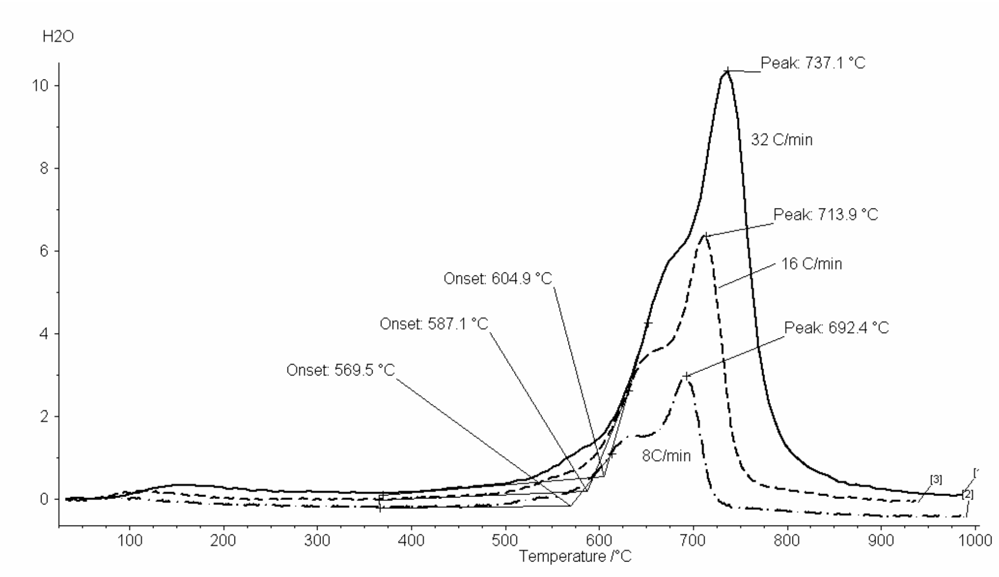

Figure 3 – Trends in H_2O Evolution for the Dehydroxylation of Chrystotile

4. Kinetic Modeling

The objective of this work was to develop a kinetic model describing the decomposition of the chrysotile mineral on heating. It was unclear from the models proposed in the literature when the forsterite phase begins to form. A second objective of this work was to clarify this point and determine if forsterite began to form during dehydroxylation or only after the recrystallization exotherm. The kinetic model developed in this investigation could be used to them predict worker exposure to chrysotile in industrial settings where the fibrous material had been used as insulation in high temperature process equipment with a known thermal history.

To develop the kinetic model describing the dehydroxylation of this chrysotile sample, the Advanced Thermokinetics Software developed by Netzsch was used [6]. For the kinetic model of the dehydroxylation reaction, the TG data was used. The DSC data was also modeled for the forsterite recrystallization but is not discussed in this report. A tabular summary of the trend of the onset of dehydroxylation from the TG data was given in Table 2. As stated, there was a strong trend of increasing onset temperatures with increasing heating rate. The small initial weight loss due to the evolution of adsorbed water was not included in the data used for kinetic modeling and the Advanced Thermokinetic Software automatically corrected the data so that the starting values were 100%.

To model the data, the Ozawa-Flynn model free analysis, given in Figure 4, was used to estimate the number of reactions suggested by the experimental data [7]. This analysis also gives estimations of the activation, E_a, and pre-exponential term, log A, for each of the reactions [7]. For the dehydroxylation data, three reactions were suggested by the model free data. The recommendation of three reaction steps can be understood by considering the thermal analysis and evolved gas data previously reported regarding the two stage nature of the dehydroxylation reaction and the impurity phases detected by evolved gas analysis signals. The first two reactions appear to relate to the two-stage behavior observed for the dehydroxylation of the chrysotile mineral. The first reaction should be related to the preferential decomposition of the fiber edges while the second reaction should be related to the decomposition of the bulk of the fiber. The final reaction is either due to the decomposition of the small magnetite, $MgCO_3$, impurity or a declining decomposition rate due to transport from the interior of the fibers.

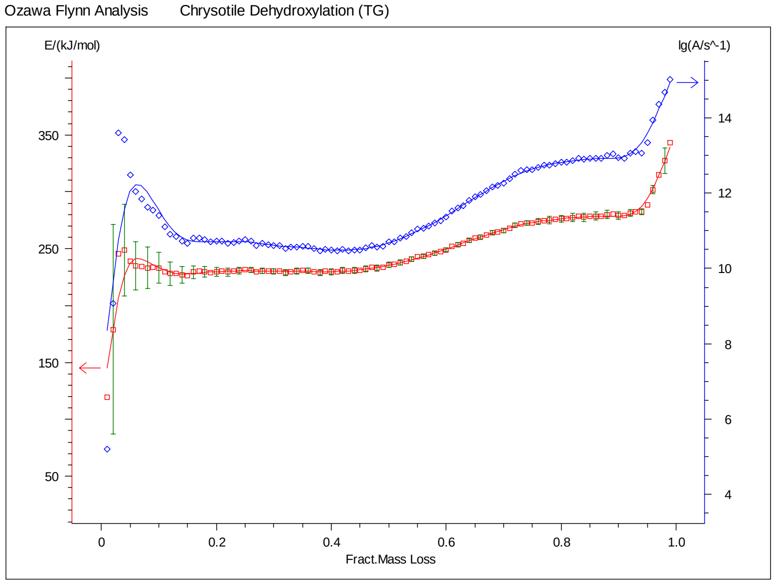

Figure 4 – Model Free Analysis of TG Kinetic Data

For the kinetic model of the dehydroxylation, the data was fit over a range of partial reaction, α, from 0.001-0.999. Three sequential reactions were required to fit the data. The overall fit was quite good with a correlation coefficient, R^2, of 0.9995. The data fit is illustrated graphically in Figure 5 where the real data and the model prediction are overplayed for comparison.

For the first two reactions that describe the two-stage dehydroxylation of the mineral, three dimensional (Jander's) diffusion equations were used to describe the data while the final reaction was fit with an Nth order reaction. A summary of the kinetic data is given in Table 3. The activation energy and pre-exponential term were much higher for the second reaction than the first reaction. This seems to correlate with the theory that the fiber edges decompose first (with a lower activation energy) and the bulk of the fiber decomposes at a high temperature (and activation energy). The first reaction only contributes a small fraction to the overall reaction while the second reaction contributes the bulk of the overall reaction.

An explanation of the final reaction needed to describe the data is somewhat less clear. A generic Nth order reaction was required to fit the data and could either represent the decomposition of the magnesite impurity or a declining rate of the dehydroxylation. What the model does not tell us is the identity of the decomposition product. To ascertain what this product is, X-ray diffraction was employed and these results will be described in a subsequent section.

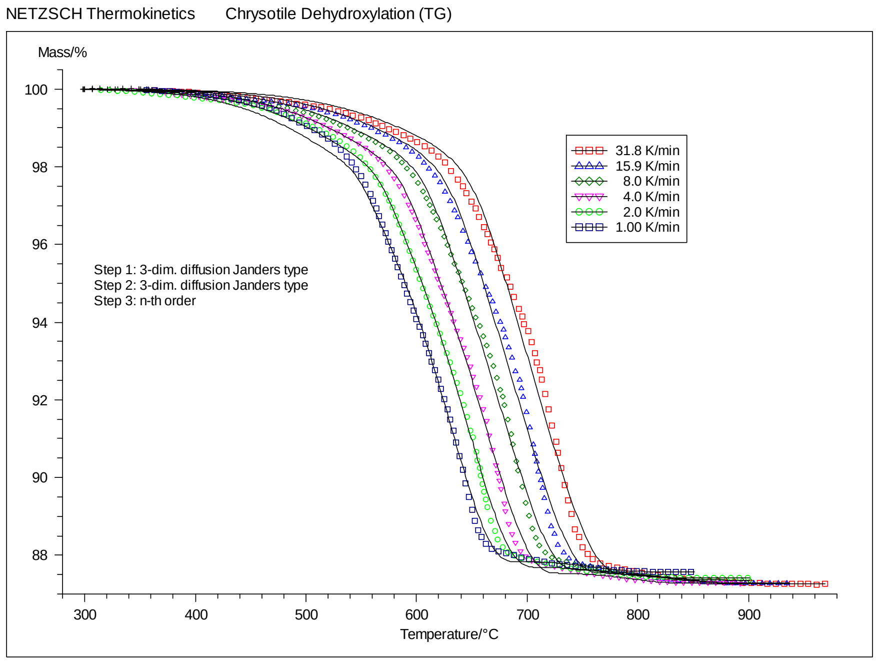

Figure 5 – Model Fit with TG Kinetic Data

Table 3 – Parameters of the Kinetic Model of the Dehydroxylation Data

Reaction Step	**1**	**2**	**3**
Reaction Type	**3 Dimensional Diffusion (Jander's)**	**3 Dimensional Diffusion (Jander's)**	**Nth order**
E_a (kJ/mol)	168	282	384
Log A (s^{-1})	7	12	16
Reaction Order			1.3
Weighting Factor	0.17	0.81	

5. Verification of the Kinetic Models

To verify the predictions of phase composition and test the kinetic model for dehydroxylation of chrysotile, large samples of the test material were heated to 600°C at a fixed heating rate of 25°C min^{-1}. One sample was heated to 600°C and allowed to cool to room temperature in the instrument. Two separate samples were maintained (soaked) at 600°C for 4 hours and 24 hours respectively. The resultant phase composition was determined by XRD. For the large samples, 300 mg of the chrysotile test material was heated in a large TG (3.4 ml) alumina crucible with a TG only sample carrier on the Netzsch 449C used for the data collection in the previous section. After heating the samples were cooled, and lightly ground in a mortar and pestle to prepare the material for X-ray diffraction analysis. Samples that had substantially dehydroxylated, very readily disintegrated in the mortar and pestle. For the samples that had not experienced a substantially degree of dehydroxylation, the particle size of the fibers was not reduced in the mortar and pestle, and these samples had to be analyzed in fiber form. The samples that maintained the fibrous habit were rotated during the diffraction analysis to limit the effects of preferential orientation of the fibers.

A comparison of the weight loss for the sample heated to 600°C for 24 hours along with the weight loss predicted by the kinetic model for the dehydroxylation of the chrysotile sample is given in Figure 6. There was some difference between the rate of weight loss between the measured data and the predicted data that can be attributed to differences in measurement configuration between the measurements used to develop the kinetic model and the large sample measurements. For the large sample measurements, a sample size of 300 mg was used while for the kinetic measurements a sample size of 25 mg was used. There were also differences in sample configuration. These differences could contribute to differences in thermal transport that resulted in the apparent differences in the rate of weight loss. Fortunately, the difference in the total weight loss between the measured and predicted data is very small.

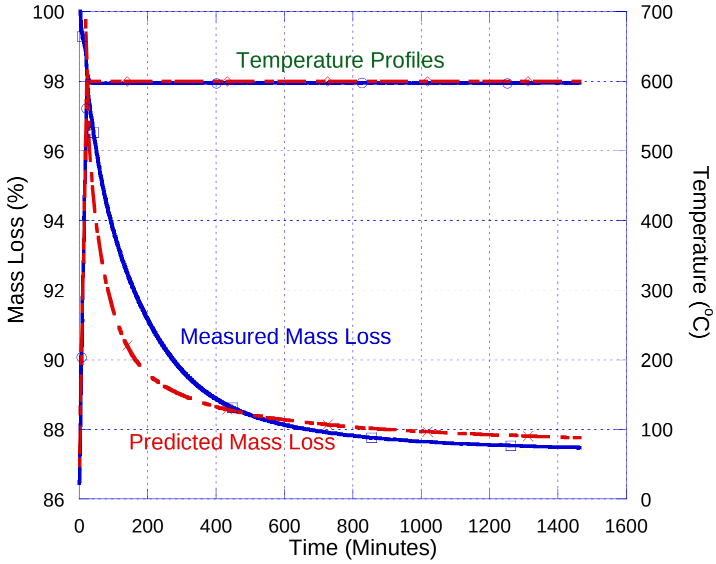

Figure 6 – Comparison of Actual and Predicted Weight Loss at 600°C

The phase composition of the samples heated to 600°C with no soak, 4 hour soak and a 24 hour soak were measured by X-ray diffraction. A comparison of the diffraction patterns for these three samples is given in Figure 7. After heating to 600°C with no soak time, diffraction peaks for chrysotile were observed. After 4 hours at 600°C, the sample was predominately amorphous, but diffraction peaks for both chrysotile and forsterite were observed. The direct observation of forsterite at a temperature below the temperature for the exotherm attributed to forsterite recrystallization was somewhat unexpected. After heating at 600°C for 24 hours, only diffraction peaks for forsterite were observed. Khorami et al. suggest forsterite as the direct product of chrysotile dehydroxylation and these observations reinforce that suggestion [3].

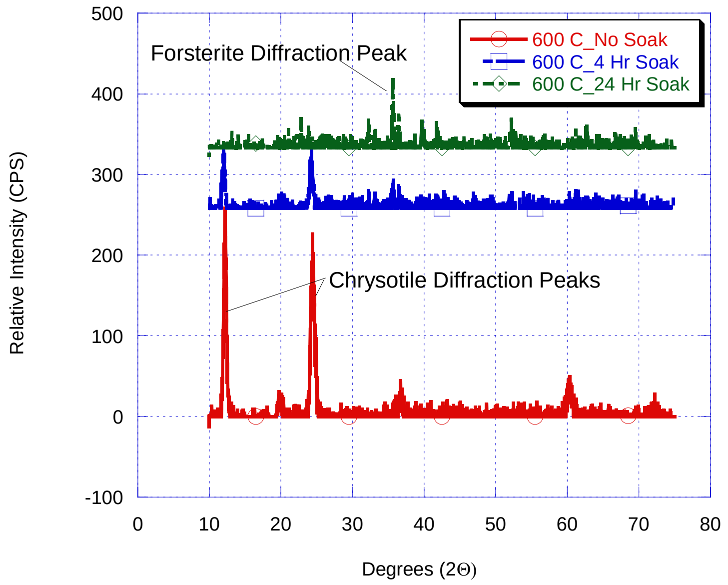

Figure 7 – Phase Development at 600°C

The Advanced Thermokinetic Software was also used to predict phase composition for the sample heated to 600°C for 24 hours. This prediction is reported in Figure 8. The model predicts that the chrysotile phase, which is labeled as A in the diagram, is consumed fairly quickly. The consumption of the chrysotile phase is followed by the emergence of a transient phase, B, which can be interpreted as an amorphous phase. Finally, the forsterite phase begins to emerge as soon as the chrysotile began to decompose, and the amount of this phase increased with exposure time. The prediction of phase development as a function of thermal treatment seems to correlate well with the trends in phase development observed in Figure 7.

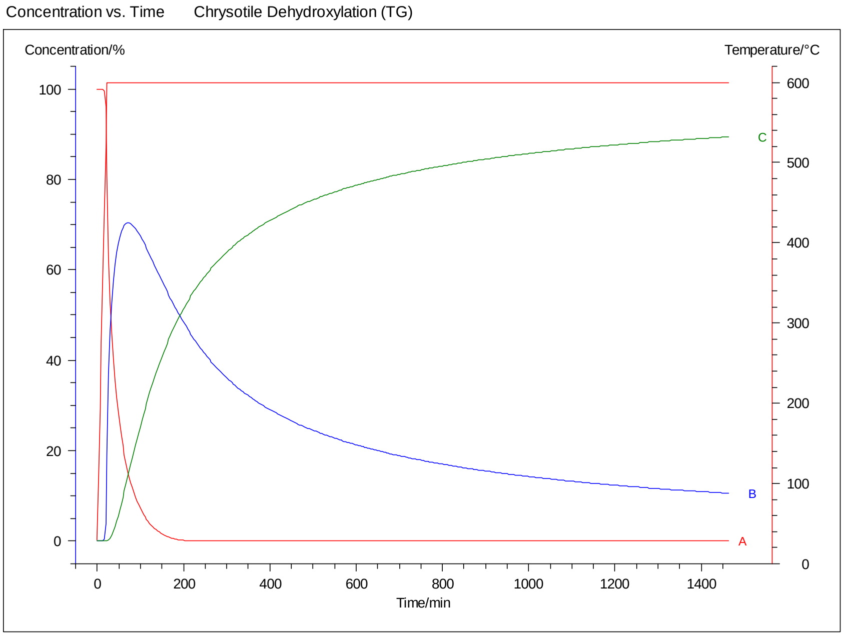

Figure 8 – Model Prediction of Phase Composition at 600°C

Finally, a Time-Temperature-Transformation (TTT) plot was derived from the kinetic model for the dehydroxylation of chrysotile. The TTT diagram is reported in Figure 9. This diagram represents, the percent of the chrysotile that will undergo dehydroxylation at a given temperature in a given exposure time. According to this diagram, dehydroxylation can be expected at temperatures as low as 400°C with very long exposure times as stated by Dodd [2].

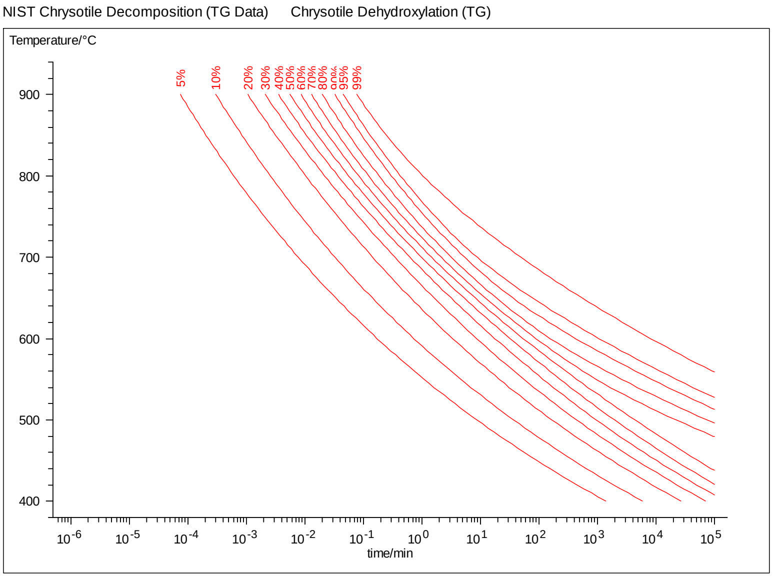

Figure 9 – Time Temperature Transformation (TTT) Diagram for the dehydroxylation of Chrysotile

6. Conclusions

A kinetic model describing the kinetics of the dehydroxylation of a chrysotile sample (NIST SRM 1866a) using thermogravimetric data was developed. The decomposition process was first studied by coupled TG/DSC/FTIR. The evolved gas analysis data from the FTIR was used to understand the thermal events observed in the TG and DSC signals. The evolved gas data was also used to rationalize the development of the kinetic model.

The kinetic model was used to predict phase composition of the chrysotile mineral under specific heat treatments. The predictions of phase distribution by the kinetic model were in good agreement with the observed phase composition of heat treated samples. It was found that forsterite is the product of chrysotile decomposition. The formation of forsterite was observed at temperatures below the temperature at where the exotherm that is attributed to forsterite recrystallization occurs.

---

[1] R. L. Virta, "Asbestos, Online Edition of the Kirk Othmer Encyclopedia of Chemical Technology, 2002.

[2] A. E. Dodd, Dictionary of Ceramics, Littelfield, Adams & Co., Great Britian (1967) 13-14.

[3]J. Khorami, D. Choquette, and F. Kimmerle, and P.K. Gallagher, Thermochimica Acta, 76, (1984) 87-96.

[4] A. Gualtieri and A. Tartaglia, Journal of the European Ceramic Society, 20, (2000) 1409-1418.

[5] R. Grimshaw, The Chemistry and Physics of Clays, TechBooks, Fairfax VA, (1971) 967-979.

[6] E. Kaisersberger, E. Post, J. Opfermann, and W.-D. Emmerich, Thermochimica Acta, 325, (1999), 25-34.

[7] J. Opfermann, E. Kaisersberger, and H. Flammersheim, Thermochimica Acta, 391 (2002) 119-127.